ARTICLE IN PRESS
JID: YICAR [m5G;August 16, 2016;17:44]

Icarus 000 (2016) 1–8

Contents lists available at ScienceDirect

Icarus

journal homepage: www.elsevier.com/locate/icarus

Low-amplitude topographic features and textures on the Moon: Initial results from detrended Lunar Orbiter Laser Altimeter (LOLA) topography

Mikhail A. Kreslavsky[a,b,*], James W. Head[c], Gregory A. Neumann[d], Maria T. Zuber[e], David E. Smith[e]

[a] Earth and Planetary Sciences, University of California, Santa Cruz, CA 95064, USA
[b] MExLab, Moscow State University of Geodesy and Cartography (MIIGAiK), Moscow, Russia
[c] Earth, Environmental and Planetary Sciences, Brown University, Providence, RI 02912, USA
[d] Solar System Exploration Division, NASA Goddard Space Flight Center, Greenbelt, MD, USA
[e] Department of Earth, Atmospheric and Planetary Sciences, MIT, Cambridge, MA, USA

ARTICLE INFO

Article history:
Received 29 January 2016
Revised 26 June 2016
Accepted 24 July 2016
Available online xxx

Keywords:
Moon, surface
Volcanism
Tectonics
Data reduction techniques

ABSTRACT

Global lunar topographic data derived from ranging measurements by the Lunar Oribter Laser Altimeter (LOLA) onboard LRO mission to the Moon have extremely high vertical precision. We use detrended topography as a means for utilization of this precision in geomorphological analysis. The detrended topography was calculated as a difference between actual topography and a trend surface defined as a median topography in a circular sliding window. We found that despite complicated distortions caused by the non-linear nature of the detrending procedure, visual inspection of these data facilitates identification of low-amplitude gently-sloping geomorphic features. We present specific examples of patterns of lava flows forming the lunar maria and revealing compound flow fields, a new class of lava flow complex on the Moon. We also highlight the identification of linear tectonic features that otherwise are obscured in the images and topographic data processed in a more traditional manner.

1. Introduction

Topography has always been an important tool in geomorphologic analysis, both terrestrial and planetary. During the last two decades new topographic data with exceptionally high vertical precision has become available: airborne lidar data (e.g., Tarolli, 2014 and references therein) for the surface of the Earth and orbital laser altimeter data for the Moon (Smith et al., 2010a, 2010b), Mars (Smith et al., 2001), and Mercury (Zuber et al., 2012). These data have revolutionized Earth and planetary geomorphology.

Despite great advances in computer data processing, visual inspection remains the main analysis tool in geomorphology. Laser altimeter data are, in a sense, too precise for easy visual perception. For example, the ranging precision of the Lunar Orbiter Laser Altimeter (LOLA) (Smith et al., 2010a, 2010b) onboard the Lunar Reconnaissance Orbiter (LRO) mission to the Moon is about 10 cm, and the topographic amplitudes on the Moon reach ~10 km, which gives an impressive dynamic range of $\sim 10^5$. Since the human eye distinguishes only a few tens of shades of grey, it is obvious that without special effort the accuracy of the data could remain unused. There are many approaches to topography visualization. For example, a widely used approach, a combination of simulated shadowing and color-coding, allows good visual perception of both large-amplitude large-scale features and smaller steep topographic features; however, such visualization still leaves some topographic information, most specifically, low-amplitude gently sloping features, beyond the limits of visual perception. Another class of approaches to the analysis of topography is based on data filtration; such methods make features of certain spatial scale visually perceptible at the expense of features of larger and/or smaller spatial scales. Removal of information about large spatial scales is referred to as "detrending", and the result is a "detrended topography".

In order to fully actualize the great potential of the LRO LOLA data, we apply a particular detrending algorithm to the LOLA topographic data for the Moon. This technique provides important new information on previously unrecognized lava flow textures and "stealth" tectonic structures in the lunar maria. We found that for features with the smallest spatial dimension of a kilometer and larger, detrended topography supersedes analysis of images

* Corresponding author at: Earth and Planetary Sciences, University of California, Santa Cruz, CA 95064, USA. Fax: +1 831 459 3074.
E-mail address: mkreslav@ucsc.edu (M.A. Kreslavsky).

http://dx.doi.org/10.1016/j.icarus.2016.07.017
0019-1035/

obtained at low Sun illumination (for example, near the lunar terminator; e.g., Lloyd and Head, 1972; Head and Lloyd, 1971, 1972a, 1972b, 1973), which has long been used for analysis of low-amplitude gently sloping morphologic features. The same detrending algorithm has been successfully applied to martian topography by Kreslavsky and Head (2002), Head et al. (2002), and Head and Marchant (2003).

In this paper we first describe the source data used, the detrending algorithm, and the rationale for its choice; we then consider the nature of the product, and illustrate the types of artifacts that can appear in the data and that, if not considered, can lead to misinterpretation. We conclude by showing selected examples of textures and features revealed in the detrended LOLA data.

2. Source data

As source data for detrended topographic maps, we use LRO LOLA data in the form of raster topographic maps available from the Planetary Data System (PDS), the so-called Gridded Data Record - GDR in the PDS terminology. The data are available in simple cylindrical projection for the entire lunar surface, and in polar azimuthal stereographic projection for both high-latitude regions. The PDS contains two versions of the data, where elevation for each grid element (pixel) is represented by either integer (with 0.5 m quantization) or by floating-point number. We used the latter version to fully employ the high ranging precision of LOLA. Elevation at each pixel had been calculated as an average of all individual elevation measurements within the pixel; pixels with no measurements were derived by interpolation between nearby pixels (Smith et al., 2010a).

There is a range of maps with different discretization (pixel size) in the PDS. Higher spatial resolution, which requires finer discretization, is desirable for interpretation; however, pixels obtained by interpolation become dominant at very fine discretization. For the simple cylindrical projection map we found the 64 pixels per degree product to have the optimal discretization, the finest discretization, under which the majority of pixels do have data (21% of all pixels had been obtained by interpolation in the data release we used). This discretization corresponds to a 474 m pixel size at the equator.

3. Detrending algorithm

The detrended elevation at each pixel was calculated as a difference between its actual elevation and the median elevation of all pixels within a circular window centered at this pixel. The window radius defines the spatial scale of the features that are considered as a global trend and thus are subject to removal. Small windows favor detection of the weakest small-size features, however, the amount of information removed from the data is huge and the amount of remaining information is tiny. For larger windows, the retained amount of information is greater, but features of interest may become obscured by clutter. We produced maps with a 5, 10, and 15 pixel window radii, which is equivalent to about a 5, 10, and 15 km diameter window at the equator. In our calculations the window radius was the same in pixels for the whole map and thus prone to map projection distortion. The impact of this distortion on visual perception of the map is minor, except for high latitudes; the high latitudes, however, are covered by the polar stereographic maps that have small distortion.

In a sense, the filtering algorithm used here is similar to widely used high-pass linear filters. The difference is that we take the median, while the linear high-pass filter takes the weighted arithmetic mean in the sliding window. Any reasonable detrending algorithm, including both our median-based and the traditional linear filters, perfectly filters out topographic features much larger than the window, preserves topographic features much smaller than the window, and inevitably distorts features comparable to the window in size. In a sense, for features somewhat smaller than the window, the median-based detrending produces less distortion, than the linear filter, as illustrated in Fig. 1. This makes the result of the median-based detrending much better for visual perception than the result of a linear high-pass filter. This was the principal reason for our choice of the median-based detrending approach.

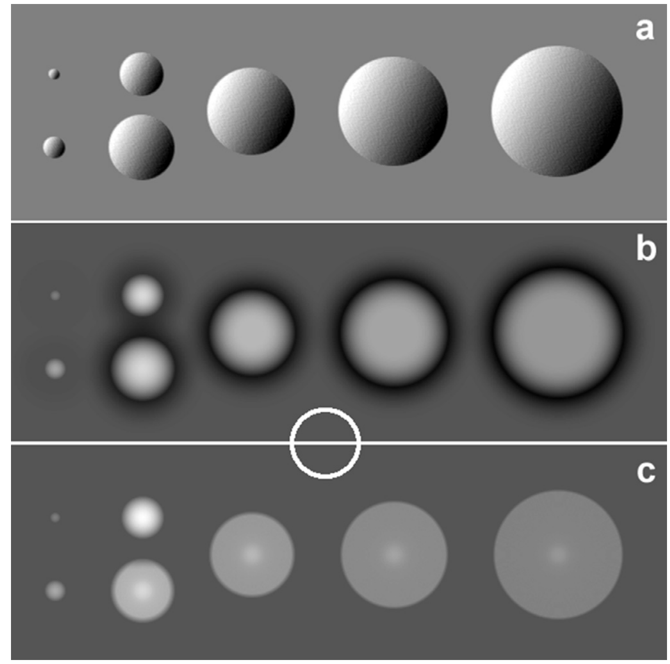

Fig. 1. Artificial topography consisting of seven similar parabolic domes rendered as artificially shaded relief (a), illumination from upper left, and results of the application of the linear high-pass filter (b) and median detrending procedure (c) rendered in a grayscale map, brighter shades denoting higher elevations. The grayscale stretch is the same in (b) and (c). White circle between (b) and (c) shows the detrending window.

The essential advantage of the median-based detrending is accompanied by several shortcomings. Due to the non-linear nature of the procedure, distortions of window-scale features produced by the median-based detrending are more complicated; for example, unlike in the case of the linear high-pass filter, in this case, a gentle tilt of the whole surface may alter the appearance of some features. The median is more computationally intensive than linear averaging, and computational feasibility requires careful implementation of the algorithm.

4. Key to interpretation of the detrending results

Artificial examples of the detrending results are shown in Figs. 1c and 2. Fig. 3 shows location of several examples of detrended topographic maps on the Moon. The maps themselves are shown in Figs. 4, 5, 7 and 8; Figs. 6 and 9 shows low-Sun photomosaics for the areas shown in Figs. 5 and 8 for comparison.

Grayscale rendition is the most suitable approach for visual analysis of the detrended topographic maps. We use a linearly stretched grayscale with brighter shades denoting topography above the trend surface, and darker shades denoting topographic lows. The use of inverse, "negative" coding is also possible and might be useful in order to improve visual perception for some applications, as well as a non-linear stretch.